

A novel approach toward finite nuclei: between *ab initio* and energy–density–functional theories

C.J. Yang,^{1,2} W.G. Jiang,¹ S. Burrello,³ and M. Grasso⁴

¹*Department of Physics, Chalmers University of Technology, SE-412 96, Göteborg, Sweden*

²*Nuclear Physics Institute of the Czech Academy of Sciences, 25069 Řež, Czech Republic*

³*Institut für Kernphysik, Technische Universität Darmstadt, 64289 Darmstadt, Germany*

⁴*Université Paris-Saclay, CNRS/IN2P3, IJCLab, 91405 Orsay, France*

We propose a novel idea to construct an effective interaction under energy–density–functional (EDF) theories which is adaptive to the enlargement of the model space. Guided by effective field theory principles, iterations of interactions as well as enlargements of the model space through particle-hole excitations are carried out for infinite nuclear matter and selected closed-shell nuclei (⁴He, ¹⁶O and ⁴⁰Ca) up to next-to-leading order. Our approach provides a new way for handling nuclear matter and finite nuclei within the same scheme, with advantages from both EDF and *ab initio* approaches.

One important challenge in the nuclear many-body problem concerns the construction of interactions. Existing state-of-the-art approaches can be mainly categorized into two extremes: one starts with bare nucleon–nucleon (NN) degrees of freedom and improves the results order by order following effective-field-theory (EFT) [1–14] through *ab initio* calculations [15–24]; the other adopts the EDF framework to build an “in medium” interaction within the self-consistent mean-field (MF) approximation and to eventually evaluate beyond MF (BMF) effects, usually employing the same interaction. However, the use of the same interaction may generate an overcounting of correlations at the BMF level. More refined methods exist to overcome this problem, such as self-energy-subtraction procedures, which are used for example in the second random-phase approximation [25].

In both approaches, which differ in the treatment of the interaction and in other aspects, the interaction is defined in a fixed model space—which stays *unchanged* throughout all considered orders.

In *ab initio* calculations, order-by-order improvable NN and few-body interactions can be constructed based on nucleonic degrees of freedom and iterated through the many-body solvers of choice. Much of the efforts have been spent on reducing the enormous model space required for the convergence of many-body calculations. Attempts to build the interactions within a sufficiently small model space have been carried out through methods of unitary transformations [26–28] or an EFT procedure which accounts for both ultraviolet and infrared truncations [29–37]. However, since *ab initio* interactions under EFT are built with a specific breakdown scale M_{hi} and a relevant momentum scale M_{lo} , one would unavoidably lose resolution when the model space is brought down below M_{hi} [38, 39]¹. In that scenario, it is ques-

tionable whether the best strategy is to insist on the original M_{lo}/M_{hi} expansion based on NN degrees of freedom. Moreover, recent studies suggest a further complication of *ab initio* approaches, that is the growing importance of three- and four-nucleon forces with the number of particles in a system [40–42].

On the other hand, as a first approximation, EDF-based approaches [43–48] reduce the many-body problem into a MF problem, where effective interactions are constructed phenomenologically within a model space corresponding to the Fermi sphere of a system. Instead of a non-perturbative treatment, approaches such as the MF Hartree-Fock approximation or BMF methods are applied (see for instance Refs. [25, 49–57]).

Though come with great simplifications, good features of *ab initio* approaches such as order-by-order improvability and predictive power are lost in the EDF-based approaches, and it is of interest to design an approach which is more balanced in-between. Inspired by recent efforts toward bridging EDF and EFT ideas [58–79], we probe in this work a novel possibility—which proposes to improve *both* the interaction and the model space order by order. Specifically, we assume there is an underlying EFT expansion where the MF results correspond to the LO contribution. Subleading corrections are then added, which contain the iterated LO interaction renormalized in an enlarged model space through particle-hole excitations. Constructing an EFT in this direction naturally leads to a novel setup which demands: (i) the interaction to be adaptive to the growth of the model space at each order, (ii) iterations of LO interactions to be performed through an in-medium propagator. This strategy offers an opportunity to eliminate model-dependence order-by-order, and was already applied to infinite matter for instance in Refs. [61, 65, 68, 78]. An attempt to include

¹ The error will be then dominated by M_{IR}/M_M instead of M_{lo}/M_{hi} (since now $M_{IR}/M_M > M_{lo}/M_{hi}$), where M_M (M_{IR})

denotes the actual resolution of the highest (infrared) scale due to the restriction of the model space.

the second-order Dyson diagrams has been probed via the calculation of the ^{16}O binding energy in Ref. [80]. However, an investigation which fully exploits the advantages of an enlarged model space and analyzes the renormalizability of various power-counting scenarios for both nuclear matter and finite nuclei is so far absent.

We present here a first study where we apply such a strategy to both matter and finite nuclei, putting the basis for a novel approach to be adopted in nuclear structure and reaction calculations. Our focus is indeed to develop a unified framework together with an order-by-order improvable and renormalizable interaction which has the potential to be applied to infinite nuclear matter and nuclei across the entire nuclear chart, as traditional EDF does.

We start by defining the Hamiltonian H_{LO} , which contains the kinetic term plus the LO interaction term V^{LO}

$$H_{LO} = \sum_i e_i \hat{n}_i + \sum_{i>j} V_{ij}^{LO}, \quad (1)$$

where e_i and \hat{n}_i are the energy and the particle-number operator for the particle i . The interaction term V_{ij}^{LO} is a two-body operator to be determined. To speculate a reasonable LO interaction under EDF, we make use of one basic requirement of EFT—the renormalizability of the observables. Studies performed for nuclear matter in Refs. [63, 64, 78] suggest that a $t_0 - t_3$ model of Skyrme-type interactions is most likely to be a suitable candidate for V^{LO} . MF calculations of Eq. (1) are straightforward for both nuclear matter and finite nuclei.

However, we do not adopt the conventional Hartree-Fock procedure here. Since the EDF effective interaction is purely phenomenological, the only way to acquire a better EDF description is to improve the effective interaction itself, if one stops at the MF level. One could then include more complicated terms, but the improvement would not be necessarily systematic. On the other hand, guided by empirical information (such as the information obtained by shell-model calculations fitted to experiments), one could start with an ansatz of the wavefunction Ψ and evaluate H_{LO} by calculating its matrix element. Note that here Ψ defines our model space at LO and does not change with the effective interaction. It was shown in Ref. [81] that reasonably good results can be obtained by directly sandwiching the Gogny interaction with a wavefunction consisting of a single-particle basis constructed in the shell model. Inspired by that, we directly define our LO model space as the shell-model wavefunction up to the highest occupied shell and calculate the expectation value of the Hamiltonian perturbatively. The ground-state (g.s.) energy of the system at LO can be written as $E_{g.s.}^{LO} = E_v + E_{coul} - t_{CM} + E_c$, with E_v, E_{coul}, E_c the energy of valence particles, the Coulomb, and the core contributions, respectively; $t_{CM} = \frac{3}{4}\hbar\omega$ is the center-

of-mass (CM) kinetic energy. In this exploratory work we only consider closed-shell nuclei, so that $E_v = 0$. The core energy can be further written as the core kinetic plus the core potential energy, that is $E_c = t_c + V_c$, where [81]

$$t_c = \sum_{j_a^c} (2T+1)(2J+1) \langle j_a^c | \hat{t} | j_a^c \rangle, \\ V_c = \sum_{j_a^c \leq j_b^c} \sum_{JT} (2T+1)(2J+1) \langle j_a^c j_b^c | JT | V^{LO} | j_a^c j_b^c | JT \rangle. \quad (2)$$

Here j_a^c, j_b^c label the single-particle orbits in the core, \hat{t} is the kinetic energy operator; J and T are the total angular momentum and isospin quantum number for each pair of interacting particles, respectively.

Note that the combination of the harmonic oscillator (HO) strength $\hbar\omega$ and N_{max} (denoting the truncation up to the highest occupied shell) provides a natural cutoff of the Fermi sphere in finite nuclei and might play a similar role as the Fermi momentum k_F in the nuclear matter case. Since our interaction is singular, without additional regulators, results in general will not converge with the increase of $\hbar\omega$. For each nucleus, there exists an optimal $\hbar\omega$ so that the shell-model basis matches the size of the nucleus. For nuclei with mass number A , the empirical $\hbar\omega \approx 45A^{-1/3} - 25A^{-2/3}$ is frequently adopted [82]. With the above equations, evaluations of the g.s. energy of ^4He , ^{16}O and ^{40}Ca using V^{LO} are straightforward. The detailed derivation is given in Refs. [80, 81] and summarized in the supplemental material, together with the form assumed by the adopted LO interaction.

We present the g.s. energies as a function of $\hbar\omega$ in Fig.1, where a $t_0 - t_3$ model of the SkP parametrization [83] is adopted for V^{LO} . LO calculations systematically provide strongly overbound nuclei with respect to experimental data, even at the empirical value of $\hbar\omega$, though the corresponding MF equation of state (EoS) for symmetric matter (SM) (shown in the inset of Fig.1) is quite satisfactory. This is not surprising judging from the simple form of the LO interaction. We have tried other $t_0 - t_3$ parametrizations, which reproduce as well the empirical SM EoS, and found that the systematic overbinding persists. On the other hand, with the $t_{1,2}$ Skyrme terms included, the MF g.s. energies obtained from SkP [83] or SLy5 [84–86] are very reasonable, with the minimum also located close to the empirical $\hbar\omega$ value.

Next, we consider NLO. Up to NLO, one has

$$E_{NLO} = E^{LO} + \langle \Psi | V_{ij}^{CT} | \Psi \rangle + E_{iter}^{NLO}, \quad (3)$$

where V_{ij}^{CT} is the higher-order contact interaction entering at NLO with its contribution evaluated at the MF level (the same way as in Eq. (2)). The structure of V_{ij}^{CT} has to be determined according to the renormalizability and the power-counting scheme. E_{iter}^{NLO} represents the contribution of the once-iterated diagrams listed in

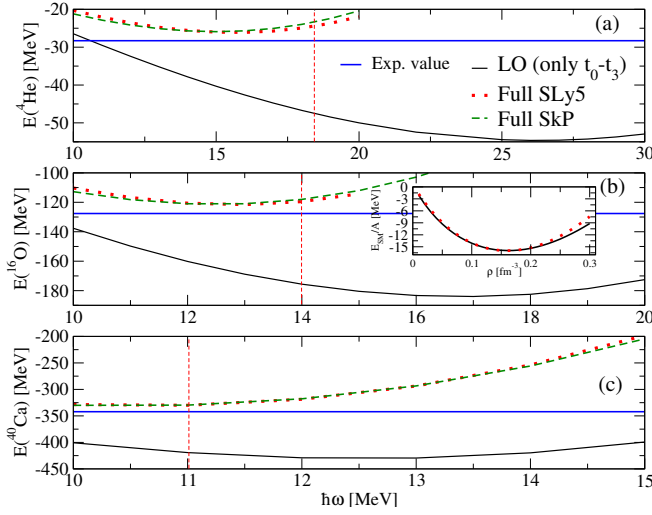


Figure 1. Ground state energies of ${}^4\text{He}$ (a), ${}^{16}\text{O}$ (b), and ${}^{40}\text{Ca}$ (c) as a function of $\hbar\omega$. Results obtained from a t_0 - t_3 model and full SLy5, and SkP functionals are plotted as black solid, red dotted, and green dashed lines, respectively. The empirical $\hbar\omega$ value for each nucleus is marked as a red vertical dashed line. The horizontal blue lines represent the experimental energies. The SM energy per particle at LO is plotted as a function of the density ρ in the inset.

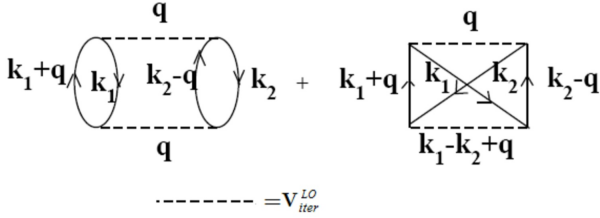


Figure 2. Once-iterated diagrams. The dashed lines stand for the interaction V_{iter}^{LO} , \mathbf{k}_1 (\mathbf{k}_2) denotes the single-particle momentum of the initial (final) state, and \mathbf{q} is the transferred momentum.

$$E_{iter}^{NLO} = \frac{f(\hbar\omega)}{4} \left[\int d^3\mathbf{k} \int d^3\mathbf{k}' \int d^3\mathbf{K} \langle \Psi(\mathbf{K}; \mathbf{k}) | V_{iter}^{LO}(\mathbf{k}; \mathbf{k}') | \psi(\mathbf{k}') \rangle G \langle \psi(\mathbf{k}') | V_{iter}^{LO}(\mathbf{k}'; \mathbf{k}) | \Psi(\mathbf{K}; \mathbf{k}) \rangle \right]_{BC}. \quad (5)$$

where

$$G = \frac{-m}{k'^2 - k^2}. \quad (6)$$

Ψ is represented in the same basis used at LO, which depends on the CM momentum $\mathbf{K} = \mathbf{k}_1 + \mathbf{k}_2 = \mathbf{k}'_1 + \mathbf{k}'_2$ and on the relative momentum \mathbf{k} . $\psi = \sum_i \phi_i$ denotes the

Fig. 2. The general form of E_{iter}^{NLO} reads [87]:

$$E_{iter}^{NLO} = -\frac{1}{4} \sum_{j_a^c \leq j_b^c, X_\alpha \leq X_\beta} \frac{|\langle j_a^c j_b^c JT | V_{iter}^{LO} | X_\alpha X_\beta JT \rangle|^2}{\varepsilon_\alpha + \varepsilon_\beta - \varepsilon_a - \varepsilon_b}, \quad (4)$$

where $j_{a(b)}^c$ are the same as in Eq. (2) because one stops at the highest occupied orbital; $X_{\alpha(\beta)}$ stands for excited states, where the summation starts at the Fermi sphere and stops at an upper limit which defines the second-order model space; $\varepsilon_i = k_i^2/2m$ is the single-particle energy of each state having momentum k_i (the effective mass is set to its bare value $m = 939$ MeV in this work). V_{iter}^{LO} denotes the part of the LO interaction which is iterated to provide the NLO contribution. A straightforward evaluation of Eq. (4) is in principle possible. However, the truncation applied to the excited states in the single-particle basis cannot be directly matched with the truncation performed for the EoS of matter in Refs. [63, 64, 78]—where a relative momentum cutoff Λ is applied. Moreover, Moshinsky transformations require all excited states $X_{\alpha,\beta}$ to be represented in terms of the HO basis², which complicates the matching between different nuclei, as they correspond to different $\hbar\omega$ and upper limit of $X_{\alpha(\beta)}$.

To produce a renormalized interaction to be easily applied to all cases, we proceed as follows. First, since excitations are governed by V_{iter}^{LO} , one can directly represent the relevant wavefunctions in relative coordinates. Let us call $\mathbf{k}_1, \mathbf{k}_2$ ($\mathbf{k}'_1, \mathbf{k}'_2$) the single-particle momenta of the initial/final (intermediate) state. Then, the incoming and outgoing momenta in relative coordinates are $\mathbf{k} = (\mathbf{k}_1 - \mathbf{k}_2)/2$, $\mathbf{k}' = (\mathbf{k}'_1 - \mathbf{k}'_2)/2 + \mathbf{q}$, where \mathbf{q} is the transferred momentum. Eq. (4) can be rewritten as

intermediate excitations, where ϕ_i can be represented by any complete basis. One caveat is that if one chooses to expand Ψ and ψ in a different basis, an overall factor $f \neq 1$ will be needed to fix the norm. To define the intermediate model space, one must truncate it either by the number of basis states or by the highest momentum. In this work, we choose the second option and adopt the free wave-packets basis so that f depends only on $\hbar\omega$. The detailed derivation leading to Eq. (5) is given in the supplemental material. Note that the conversion of initial/final and intermediate single-particle-basis states (which are also restricted as mentioned before) to relative

² Alternatively, one could go through extra processes which involve the decomposition of the chosen basis into the HO one [88, 89].

coordinates results in a boundary condition (BC) which couples k_F to new variables \mathbf{k} , \mathbf{k}' and \mathbf{K} . The 3-folded integral under the same BC has been carried out to obtain the second-order EoS [65, 87], and is to be carried out in a similar manner in Eq. (5). However, unlike the nuclear matter case—where a clear definition of Fermi momentum is possible— k_F is not clearly given in finite nuclei. In the nuclear matter case, the radial integral dk is truncated by $k \in [0, k_F]$. On the other side, in finite nuclei, the same integrals are carried out through $k \in [0, \infty]$. However, the shell structure (the LO wavefunctions of a nucleus at a chosen $\hbar\omega$) provides a natural truncation analogous to k_F . To proceed, we interpret k_F in finite nuclei to be the highest momentum each wavefunction can access. The procedure to extract k_F in a finite nucleus is thus the following. First, we evaluate the g.s. energy at the MF level and separate the contributions from the t_0 , the t_3 , and the V^{CT} terms for each nucleus. Then, we compare the ratios $\frac{\langle t_0 \rangle}{\langle t_3 \rangle}$ and $\frac{\langle t_0 \rangle}{\langle V^{CT} \rangle}$ to their corresponding values in SM. The ratios in nuclear matter depend on k_F , whereas the same ratios in finite nuclei are related to their shell structure. By requiring the same ratios between finite nuclei and nuclear matter, we can extract the corresponding k_F for ${}^4\text{He}$, ${}^{16}\text{O}$ and ${}^{40}\text{Ca}$ under various $\hbar\omega$ values. The resulting k_F are listed in Table I. One can see that a heavier nucleus (and

$\hbar\omega$ (MeV)	11	12	13	14	15	16	17	18
k_F of ${}^4\text{He}$	0.90	0.95	0.98	1.02	1.05	1.08	1.12	1.15
k_F of ${}^{16}\text{O}$	1.08	1.13	1.18	1.22	1.26	1.30	1.34	1.38
k_F of ${}^{40}\text{Ca}$	1.25	1.37	1.35	1.40	1.45	1.49	1.54	1.58

Table I. k_F (in unit: fm^{-1}) for ${}^4\text{He}$, ${}^{16}\text{O}$ and ${}^{40}\text{Ca}$ under various $\hbar\omega$.

a larger $\hbar\omega$) naturally corresponds to a higher k_F . We have tried several interactions having different values of α (the power of the density in the t_3 term). We have found a very weak spreading ($\leq 1\%$ variations) between the values of k_F obtained by using such interactions in the matching of the ratios.

Once k_F is known, we have all the ingredients to perform actual calculations. In Refs. [64, 78], the full $t_0 - t_3$ LO interaction is iterated to generate E_{iter}^{NLO} for nuclear matter. The same procedure can be performed in principle in Eq. (5) for finite nuclei. However, some conceptual subtleties arise regarding how to account for the density ρ when one considers the fluctuation of the wavefunctions due to the intermediate excitations. In fact, in conventional EDF approaches with a density-dependent term included (for example the t_3 term of Skyrme interactions), the interaction does not correspond to a genuine Hamiltonian. The iteration of this term generates a conceptual drawback and may lead to technical problems such as divergences in BMF calculations for nuclei [90–92]. Therefore, we choose not to iterate the t_3 part of the

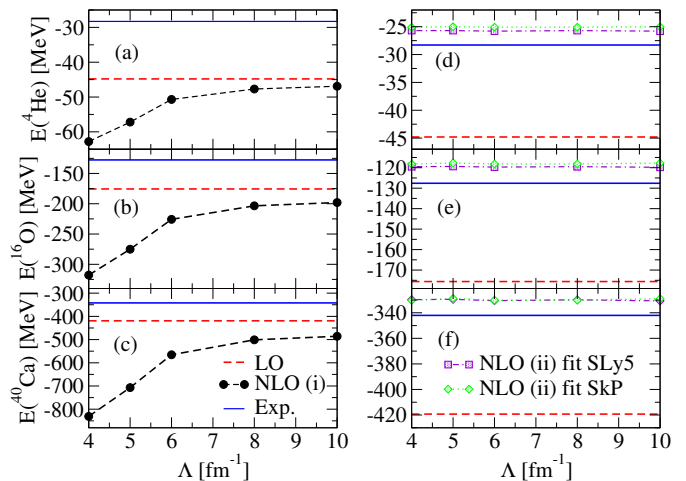


Figure 3. Ground state energies up to NLO for ${}^4\text{He}$ ((a) and (d)), ${}^{16}\text{O}$ ((b) and (e)), and ${}^{40}\text{Ca}$ ((c) and (f)), as a function of Λ . Results are obtained with the empirical values $\hbar\omega = 17, 14, 11$ MeV, respectively. The labels (i) and (ii) refer to the two prescriptions described in the main text.

interaction in this work.

In the following, we perform two types of NLO calculations:

- (i) Only the t_0 part of the LO interaction is iterated, and $V^{CT} = C(1 + x_c P_\sigma)$.
- (ii) Same as (i), but with additional $V_{ii}^{CT} = \frac{1}{2}t_1(1 + x_1 P_\sigma)(\mathbf{k}'^2 + \mathbf{k}^2) + t_2(1 + x_2 P_\sigma)\mathbf{k}' \cdot \mathbf{k}$, that is, the Skyrme-type $t_{1,2}$ terms are added.

Note that the above interactions are Skyrme-like, and $P_\sigma = (1 + \sigma_1\sigma_2)/2$ is the spin-exchange operator. We treat C , x_c , α , $t_{1,2}$, and $x_{1,2}$ as the low-energy constants (LECs) in EFT, and we choose to renormalize them to reproduce the SLy5 SM and neutron matter (NM) EoSs. The LECs, the χ^2 values and the resulting EoSs are given in the supplemental material. Predictions on g.s. energies of ${}^4\text{He}$, ${}^{16}\text{O}$, and ${}^{40}\text{Ca}$, evaluated up to NLO with $\Lambda = 4 - 10 \text{ fm}^{-1}$, are given in Fig.3. As one can see, the pathological overbinding trend at LO seems to persist under the prescription (i). In fact, already in the uniform case, it is very difficult to obtain good simultaneous fits for both SM and NM. Thus, without the entrance of new k_F -dependencies in the EoS of matter (other than terms behave asymptotically $\sim k_F^4$ and proportional to t_0^2) at NLO, one does not observe any improvement from LO to NLO for both the EoS of matter and finite nuclei. Since one expects results up to NLO to be better than LO in a consistent EFT, something must be missing under prescription (i). Nevertheless, the NLO renormalizability is satisfied—which is reflected in the converging pattern of NLO (i) results against Λ in Fig.3. A real improvement is achieved by the prescription (ii), where a reasonable re-

production of the experimental binding is achieved with the inclusion of the $t_{1,2}$ terms. Note that, instead of fine-tuning the LECs, our focus here is to demonstrate an approach which includes subleading contributions—a non-trivial effect to structure of nuclei—can work as good as those best-fitted MF Skyrmes, so that we are one step further to the elimination of model-dependence. We found that one could keep in practice the SkP or SLy5 values for $t_{1,2,3}$, $x_{1,2,3}$, and α . By just tuning t_0 , x_0 , C , and x_c to the empirical EoSs, we are able to obtain satisfactory results as shown in Fig.3. This suggests that the t_1 , t_2 terms are indeed indispensable, as indicated by many phenomenological studies.

M_{hi} and M_{lo} in our proposed scheme can be speculated as follows. Since the typical low-momentum scale M_{lo} spans from 0 to k_F —which varies with the number of nucleons A in a nucleus—a successful EFT arrangement of observables up to NLO in term of powers series in (M_{lo}/M_{hi}) suggests that M_{hi} has the following properties:

- It is at least larger than k_F , and depends on the number of particles A .
- It depends on N_{max} and $\hbar\omega$, at least for those nuclei where central densities are lower than the saturation density of SM. Let us denote by A_s typical A values for which nuclei reach the saturation density in their central region. Then M_{hi} increases with A for $A < A_s$.

The breakdown scale has a functional form $M_{hi}(A, \hbar\omega)$. For $A < A_s$, the asymptotic form of the EFT expansion is $\frac{M_{lo}}{M_{hi}} \sim \frac{k}{\beta k_F(A)}$, where k is the characteristic center-of-mass momentum scale and $\beta \gtrsim 1$. On the other hand, $\beta k_F(A) \sim \bar{M}_{hi}$, that is, becomes a constant for $A > A_s$, where \bar{M}_{hi} is a hard breakdown scale to be extracted by a Lepage-like plot [38, 39] from NLO and next-to-next-to-leading order (NNLO) results; $\frac{2}{3\pi^2} \bar{M}_{hi}^3$ and $\frac{1}{3\pi^2} \bar{M}_{hi}^3$ correspond to the highest density ρ for which one can trust the EoS of SM and NM, respectively (for example, twice the saturation density of SM).

In summary, we provide a novel framework to include BMF correlations order by order. With a reliable extraction of k_F , the treatment of finite nuclei and nuclear matter can be performed on the same footing. Investigations up to NLO are performed for ${}^4\text{He}$, ${}^{16}\text{O}$, ${}^{40}\text{Ca}$ and for nuclear matter for the first time. Our work serves as a starting point toward an EFT-based description of nuclei across the entire nuclear chart. Many interesting future works including the treatment of higher-order correlations and a full EFT power-counting analysis are in progress.

Acknowledgements. This work was supported by the Czech Science Foundation GACR grant 19-19640S, and the Swedish Research Council (Grant number 2017-04234), the European Research Council (ERC) under

the European Union’s Horizon 2020 research and innovation programme (Grant agreement number 758027). The computations of the research used resources provided by the Swedish National Infrastructure for Computing (SNIC) at Chalmers Centre for Computational Science and Engineering (C3SE), and the National Supercomputer Centre (NSC) partially funded by the Swedish Research Council. S. B. acknowledges support from the Alexander von Humboldt foundation.

-
- [1] S. Weinberg, *Physics Letters B* **251**, 288 (1990).
 - [2] S. Weinberg, *Nuclear Physics B* **363**, 3 (1991).
 - [3] C. Ordóñez, L. Ray, and U. van Kolck, *Physical Review Letters* **72**, 1982 (1994).
 - [4] C. Ordóñez, L. Ray, and U. van Kolck, *Physical Review C* **53**, 2086 (1996).
 - [5] E. Epelbaum, W. Glöckle, and U.-G. Meissner, *Nuclear Physics A* **637**, 107–134 (1998).
 - [6] E. Epelbaum, W. Glöckle, and U.-G. Meissner, *Nuclear Physics A* **671**, 295–331 (2000).
 - [7] D. Entem and R. Machleidt, *Physics Letters B* **524**, 93–98 (2002).
 - [8] D. R. Entem and R. Machleidt, *Physical Review C* **66** (2002), 10.1103/physrevc.66.014002.
 - [9] E. Epelbaum, W. Glöckle, and U.-G. Meissner, *Nuclear Physics A* **747**, 362–424 (2005).
 - [10] E. Epelbaum, H. Krebs, and U. G. Meißner, *Eur. Phys. J. A* **51**, 53 (2015), arXiv:1412.0142 [nucl-th].
 - [11] U. V. Kolck, *Progress in Particle and Nuclear Physics* **43**, 337–418 (1999).
 - [12] P. F. Bedaque and U. V. Kolck, *Annual Review of Nuclear and Particle Science* **52**, 339–396 (2002).
 - [13] E. Epelbaum, H.-W. Hammer, and U.-G. Meissner, *Reviews of Modern Physics* **81**, 1773–1825 (2009).
 - [14] H.-W. Hammer, S. König, and U. van Kolck, *Reviews of Modern Physics* **92** (2020), 10.1103/revmodphys.92.025004.
 - [15] W. H. Dickhoff and C. Barbieri, *Prog. Part. Nucl. Phys.* **52**, 377 (2004).
 - [16] D. Lee, *Progress in Particle and Nuclear Physics* **63**, 117 (2009).
 - [17] S. K. Bogner, R. J. Furnstahl, and A. Schwenk, *Prog. Part. Nucl. Phys.* **65**, 94 (2010).
 - [18] B. R. Barrett, P. Navrátil, and J. P. Vary, *Prog. Part. Nucl. Phys.* **69**, 131 (2013).
 - [19] A. Carbone, A. Cipollone, C. Barbieri, A. Rios, and A. Polls, *Phys. Rev. C* **88**, 054326 (2013), arXiv:1310.3688 [nucl-th].
 - [20] G. Hagen, T. Papenbrock, M. Hjorth-Jensen, and D. J. Dean, *Rep. Prog. Phys.* **77**, 096302 (2014).
 - [21] H. Hergert, S. Bogner, T. Morris, A. Schwenk, and K. Tsukiyama, *Physics Reports* **621**, 165 (2016), memorial Volume in Honor of Gerald E. Brown.
 - [22] J. Carlson, S. Gandolfi, F. Pederiva, S. C. Pieper, R. Schiavilla, K. E. Schmidt, and R. B. Wiringa, *Rev. Mod. Phys.* **87**, 1067 (2015).
 - [23] N. Barnea, W. Leidemann, and G. Orlandini, *Nuclear Physics A* **650**, 427 (1999).
 - [24] W. Glöckle, H. Witala, D. Hüber, H. Kamada, and

- J. Golak, *Physics Reports* **274**, 107 (1996).
- [25] D. Gambacurta, M. Grasso, and J. Engel, *Phys. Rev. C* **92**, 034303 (2015).
- [26] R. Roth, A. Calci, J. Langhammer, and S. Binder, *Phys. Rev. C* **90**, 024325 (2014).
- [27] S. K. Bogner, T. T. S. Kuo, and A. Schwenk, *Physics Reports* **386**, 1 (2003).
- [28] S. K. Bogner, R. J. Furnstahl, and R. J. Perry, *Phys. Rev. C* **75**, 061001 (2007).
- [29] I. Stetcu, B. R. Barrett, P. Navrátil, and J. P. Vary, *Phys. Rev. C* **71**, 044325 (2005).
- [30] I. Stetcu, B. R. Barrett, and U. van Kolck, *Physics Letters B* **653**, 358 (2007).
- [31] I. Stetcu, B. R. Barrett, U. van Kolck, and J. P. Vary, *Phys. Rev. A* **76**, 063613 (2007).
- [32] I. Stetcu, J. Rotureau, B. R. Barrett, and U. van Kolck, *Journal of Physics G: Nuclear and Particle Physics* **37**, 064033 (2010).
- [33] J. Rotureau, I. Stetcu, B. R. Barrett, M. C. Birse, and U. van Kolck, *Phys. Rev. A* **82**, 032711 (2010).
- [34] I. Stetcu, J. Rotureau, B. R. Barrett, and U. van Kolck, *Annals of Physics* **325**, 1644 (2010).
- [35] J. Rotureau, I. Stetcu, B. R. Barrett, and U. van Kolck, *Phys. Rev. C* **85**, 034003 (2012).
- [36] S. Binder, A. Ekström, G. Hagen, T. Papenbrock, and K. A. Wendt, *Phys. Rev. C* **93**, 044332 (2016).
- [37] X. Zhang, S. Stroberg, P. Navrátil, C. Gwak, J. Melendez, R. Furnstahl, and J. Holt, *Phys. Rev. Lett.* **125**, 112503 (2020), [arXiv:2004.13575 \[nucl-th\]](#).
- [38] H. W. Griefhammer, In 8th International Workshop on Chiral Dynamics (CD) Pisa, Italy, June 29-July 3, CD2015 PoS(CD15)104, [arXiv:1511.00490v3 \[nucl-th\]](#) (2015).
- [39] H. W. Griefhammer, *European Physical Journal A* **56** (2020), [10.1140/epja/s10050-020-00129-5](#).
- [40] C. J. Yang, A. Ekström, C. Forssén, and G. Hagen, *Phys. Rev. C* **103**, 054304 (2021), [arXiv:2011.11584 \[nucl-th\]](#).
- [41] C. J. Yang, *European Physical Journal A* **56**, 96 (2020).
- [42] C. J. Yang, A. Ekström, C. Forssén, G. Hagen, G. Rupak, and U. van Kolck, (2021), [arXiv:2109.13303 \[nucl-th\]](#).
- [43] P. Hohenberg and W. Kohn, *Phys. Rev.* **136**, B864 (1964).
- [44] W. Kohn and L. J. Sham, *Phys. Rev.* **140**, A1133 (1965).
- [45] W. Kohn, *Rev. Mod. Phys.* **71**, 1253 (1999).
- [46] R. M. Dreizler and E. K. U. Gross, *Density Functional Theory* (Springer Berlin Heidelberg, 1990).
- [47] R. G. Parr and W. Yang, *Density-functional theory of atoms and molecules* (Clarendon, Oxford, 1989).
- [48] T. Takao, *Density Functional Theory in Quantum Chemistry* (Springer, Tokyo, 2014).
- [49] D. Gambacurta, M. Grasso, and J. Engel, *Phys. Rev. Lett.* **125**, 212501 (2020).
- [50] C. Robin and E. Litvinova, *Phys. Rev. C* **98**, 051301 (2018).
- [51] C. Robin and E. Litvinova, *Phys. Rev. Lett.* **123**, 202501 (2019).
- [52] Y. F. Niu, G. Colò, and E. Vigezzi, *Phys. Rev. C* **90**, 054328 (2014).
- [53] G. Colò, P. F. Bortignon, M. Brenna, X. Roca-Maza, E. Vigezzi, K. Moghrabi, M. Grasso, and K. Mizuyama, *Phys. Scripta* **89**, 054006 (2014).
- [54] G. Colò, H. Sagawa, and P. F. Bortignon, *Phys. Rev. C* **82**, 064307 (2010).
- [55] S. Burrello, J. Bonnard, and M. Grasso, *Phys. Rev. C* **103**, 064317 (2021).
- [56] S. Burrello, M. Colonna, G. Colò, D. Lacroix, X. Roca-Maza, G. Scamps, and H. Zheng, *Phys. Rev. C* **99**, 054314 (2019).
- [57] S. Burrello, M. Colonna, and H. Zheng, *Frontiers in Physics* **7**, 53 (2019).
- [58] H. Hammer and R. Furnstahl, *Nucl. Phys. A* **678**, 277 (2000), [arXiv:nucl-th/0004043](#).
- [59] N. Kaiser, *J. Phys. G* **42**, 095111 (2015), [arXiv:1505.07095 \[nucl-th\]](#).
- [60] N. Kaiser, *Eur. Phys. J. A* **53**, 104 (2017), [arXiv:1703.07745 \[nucl-th\]](#).
- [61] K. Moghrabi, M. Grasso, G. Colo, and N. Van Giai, *Phys. Rev. Lett.* **105**, 262501 (2010), [arXiv:1012.3097 \[nucl-th\]](#).
- [62] K. Moghrabi, (2016), [arXiv:1607.05829 \[nucl-th\]](#).
- [63] C. J. Yang, M. Grasso, K. Moghrabi, and U. van Kolck, *Phys. Rev. C* **95**, 054325 (2017), [arXiv:1312.5949 \[nucl-th\]](#).
- [64] C. Yang, M. Grasso, and D. Lacroix, *Phys. Rev. C* **94**, 031301 (2016), [arXiv:1604.06587 \[nucl-th\]](#).
- [65] C. Yang, M. Grasso, X. Roca-Maza, G. Colò, and K. Moghrabi, *Phys. Rev. C* **94**, 034311 (2016), [arXiv:1604.06278 \[nucl-th\]](#).
- [66] D. Lacroix, A. Boulet, M. Grasso, and C.-J. Yang, *Phys. Rev. C* **95**, 054306 (2017), [arXiv:1704.08454 \[nucl-th\]](#).
- [67] M. Grasso, D. Lacroix, and C. Yang, *Phys. Rev. C* **95**, 054327 (2017), [arXiv:1704.08510 \[nucl-th\]](#).
- [68] C. J. Yang, M. Grasso, and D. Lacroix, *Phys. Rev. C* **96**, 034318 (2017), [arXiv:1706.00258 \[nucl-th\]](#).
- [69] J. Bonnard, M. Grasso, and D. Lacroix, *Phys. Rev. C* **101**, 064319 (2020), [arXiv:2001.08082 \[nucl-th\]](#).
- [70] M. Grasso, *Prog. Part. Nucl. Phys.* **106**, 256 (2019), [arXiv:1811.01039 \[nucl-th\]](#).
- [71] J. Bonnard, M. Grasso, and D. Lacroix, *Phys. Rev. C* **98**, 034319 (2018), [arXiv:1806.01084 \[nucl-th\]](#).
- [72] H. Gil, P. Papakonstantinou, C. H. Hyun, T.-S. Park, and Y. Oh, *Acta Phys. Polon. B* **48**, 305 (2017), [arXiv:1611.04257 \[nucl-th\]](#).
- [73] H. Gil, Y. Oh, C. H. Hyun, and P. Papakonstantinou, *New Phys. Sae Mulli* **67**, 456 (2017).
- [74] H. Gil, P. Papakonstantinou, C. H. Hyun, and Y. Oh, *JPS Conf. Proc.* **20**, 011041 (2018).
- [75] H. Gil, Y.-M. Kim, C. H. Hyun, P. Papakonstantinou, and Y. Oh, *Phys. Rev. C* **100**, 014312 (2019), [arXiv:1903.04123 \[nucl-th\]](#).
- [76] H. Gil, Y.-M. Kim, P. Papakonstantinou, and C. Ho, *Phys. Rev. C* **103**, 034330 (2021), [arXiv:2010.13354 \[nucl-th\]](#).
- [77] R. J. Furnstahl, *Eur. Phys. J. A* **56**, 85 (2020), [arXiv:1906.00833 \[nucl-th\]](#).
- [78] S. Burrello, M. Grasso, and C.-J. Yang, *Physics Letters B* **811**, 135938 (2020).
- [79] F. Marino, C. Barbieri, A. Carbone, G. Colò, A. Lovato, F. Pederiva, X. Roca-Maza, and E. Vigezzi, *Phys. Rev. C* **104**, 024315 (2021).
- [80] M. Brenna, G. Colò, and X. Roca-Maza, *Physical Review C* **90** (2014), [10.1103/physrevc.90.044316](#).
- [81] W. G. Jiang, B. S. Hu, Z. H. Sun, and F. R. Xu, *Physical Review C* **98** (2018), [10.1103/physrevc.98.044320](#).
- [82] J. Blomqvist and A. Molinari, *Nucl. Phys. A* **106**, 545 (1968).

- [83] J. Dobaczewski, H. Flocard, and J. Treiner, *Nuclear Physics A* **422**, 103 (1984).
- [84] E. Chabanat, P. Bonche, P. Haensel, J. Meyer, and R. Schaeffer, *Nuclear Physics A* **627**, 710 (1997).
- [85] E. Chabanat, P. Bonche, P. Haensel, J. Meyer, and R. Schaeffer, *Nuclear Physics A* **635**, 231 (1998).
- [86] E. Chabanat, P. Bonche, P. Haensel, J. Meyer, and R. Schaeffer, *Nucl. Phys. A* **635**, 231 (1998), [Erratum: *Nucl.Phys.A* 643, 441–441 (1998)].
- [87] K. Davies and M. Baranger, *Nucl. Phys. A* **120**, 254 (1968).
- [88] G. Papadimitriou, B. R. Barrett, J. Rotureau, N. Michel, and M. Płoszajczak, *EPJ Web of Conferences* **66**, 02006 (2014).
- [89] G. Papadimitriou, J. Rotureau, N. Michel, M. Płoszajczak, and B. R. Barrett, *Physical Review C* **88** (2013), 10.1103/physrevc.88.044318.
- [90] D. Lacroix, T. Duguet, and M. Bender, *Phys. Rev. C* **79**, 044318 (2009).
- [91] M. Bender, T. Duguet, and D. Lacroix, *Phys. Rev. C* **79**, 044319 (2009).
- [92] T. Duguet, M. Bender, K. Bennaceur, D. Lacroix, and T. Lesinski, *Phys. Rev. C* **79**, 044320 (2009).
- [93] R. Lawson, *Theory of the nuclear shell model* (Clarendon Press, Oxford, 1980).

SUPPLEMENTAL MATERIAL

**TWO-BODY MATRIX ELEMENTS AT
MEAN-FIELD LEVEL**

In the shell model, the j - j coupling scheme is commonly adopted. However, the two-body Skyrme- or Gogny-type effective interactions operate in the L - S coupling (partial-wave) scheme. Therefore, the following transformation is needed[93],

$$\begin{aligned} |(n_a l_a j_a)(n_b l_b j_b) J J_z\rangle &= \sum_{\lambda S} \sum_{\mu S_z} \gamma_{\lambda S}^{(J)}(j_a l_a; j_b l_b) \langle \lambda \mu S S_z | J J_z \rangle \\ &\times |(n_a l_a m_a)(n_b l_b m_b) \lambda \mu \rangle | S S_z \rangle, \end{aligned} \quad (7)$$

where $\langle \lambda \mu S S_z | J J_z \rangle$ are the standard Clebsch-Gordan coefficients and

$$\begin{aligned} \gamma_{\lambda S}^{(J)}(j_a l_a; j_b l_b) &= \sqrt{(2j_a + 1)(2j_b + 1)(2S + 1)(2\lambda + 1)} \\ &\times \begin{Bmatrix} l_a & 1/2 & j_a \\ l_b & 1/2 & j_b \\ \lambda & S & J \end{Bmatrix}. \end{aligned} \quad (8)$$

Here J and J_z denote the total angular momentum and its z -component, respectively, and S and S_z are the total intrinsic spin and its z -component, respectively.

One could rewrite the two-particle wavefunctions in the laboratory coordinates with quantum numbers $(J J_z T)$ in terms of wavefunctions in relative coordinates, that is,

$$\begin{aligned} &| (n_a l_a j_a)(n_b l_b j_b) J J_z T \rangle \\ &= \sum_{nlNL} \sum_{mM} \sum_{\mu S_z} \sum_{\lambda S} \gamma_{\lambda S}^{(J)}(j_a l_a; j_b l_b) \frac{1 - (-1)^{S+T+l}}{\sqrt{2(1 + \delta_{n_a n_b} \delta_{l_a l_b} \delta_{j_a j_b})}} \\ &\times M_\lambda(nlNL; n_a l_a n_b l_b) \langle l m L M | \lambda \mu \rangle \langle \lambda \mu S S_z | J J_z \rangle \\ &\times | n l m \rangle | N L M \rangle | S S_z \rangle | T \rangle, \end{aligned} \quad (9)$$

where $|T\rangle$ is the two-particle isospin eigenstate with a total isospin T . Finally, the full expression of the two-body

matrix element of an effective interaction V_{NN} reads

$$\begin{aligned} &\langle (n_a l_a j_a)(n_b l_b j_b) J J_z T | V_{NN} | (n_c l_c j_c)(n_d l_d j_d) J J_z T \rangle \\ &= \sum_{n'l'N'L'} \sum_{nlNL} \sum_{m'M'} \sum_{mM} \sum_{\mu'S'_z} \sum_{\mu S_z} \sum_{\lambda'S'} \sum_{\lambda S} \tilde{\gamma}_{\lambda'S'}^{(J)}(j_a l_a; j_b l_b) \\ &\times \tilde{\gamma}_{\lambda S}^{(J)}(j_c l_c; j_d l_d) M_{\lambda'}(n'l'N'L'; n_a l_a n_b l_b) \\ &\times M_\lambda(nlNL; n_c l_c n_d l_d) \langle l' m' L' M' | \lambda' \mu' \rangle \\ &\times \langle \lambda' \mu' S' S'_z | J J_z \rangle \langle l m L M | \lambda \mu \rangle \langle \lambda \mu S S_z | J J_z \rangle \\ &\times \langle T | \langle S' S'_z | \langle N' L' M' | \langle n' l' m' | V_{NN} | n l m \rangle | N L M \rangle \\ &\times | S S_z \rangle | T \rangle, \end{aligned} \quad (10)$$

with $\tilde{\gamma}_{\lambda S}^{(J)}(j_a l_a; j_b l_b) = \frac{1 - (-1)^{S+T+l}}{\sqrt{2(1 + \delta_{n_a n_b} \delta_{l_a l_b} \delta_{j_a j_b})}} \gamma_{\lambda S}^{(J)}(j_a l_a; j_b l_b)$, where symbols with prime refer to the left vector. Note that if V_{NN} consists only of s -waves, then the kernel $\langle n' l' m' | V_{NN} | n l m \rangle$ can be further simplified into:

$$\begin{aligned} &\langle n' 0 m' | V_{NN,12} | n 0 m \rangle \\ &= \frac{1}{2\pi^2} \int_0^\infty p^2 dp \int_0^\infty p'^2 dp' \psi_{n' 0 m'}(p) V_{0,0s=j}(p, p') \psi_{n 0 m}(p'). \end{aligned} \quad (11)$$

Here $V_{0,0s=j}(p, p')$ is the s -wave component of V_{NN} , and $\psi_{nl=0m}$ is the standard Harmonic oscillator (HO) wavefunction with quantum numbers n, l, m . In the above expression, we have assumed that V_{NN} is density independent. For density-dependent effective interactions (such as the Skyrme one), one may follow Eqs. (4)-(7) in Ref.[81] to perform the integral over the CM coordinate space $\mathbf{R} = (\mathbf{r}_1 + \mathbf{r}_2)/2$ and to evaluate the matrix element of $\langle N' L' M' | \hat{\rho}(\mathbf{R}) | N L M \rangle$. Here $\hat{\rho}(\mathbf{R})$ is proportional to the modular square of the CM part of the wavefunction, with details given in Ref.[81].

The LO interaction adopted in this work has the following form:

$$V_{12}^{LO} = \delta(\mathbf{r}_1 - \mathbf{r}_2) t_0 (1 + x_0 P_\sigma) + \delta(\mathbf{r}_1 - \mathbf{r}_2) \frac{t_3}{6} (1 + x_3 P_\sigma) \rho^\alpha, \quad (12)$$

where t_0, t_3, x_0, x_3 , and α are parameters, $\rho = \rho(\frac{\mathbf{r}_1 + \mathbf{r}_2}{2})$ is the density, and $P_\sigma = (1 + \sigma_1 \sigma_2)/2$ is the spin-exchange operator.

Note that Eq. (10) can be reduced to a simpler form in the case of infinity nuclear matter, where the system becomes homogeneous so that it can be described by a Fermi gas with wavefunction Ψ consisting of free wavepackets u_k labelled by the momentum k . Within a box volume Ω , Eq. (10) becomes

$$\sum_{u_k, u_p} \sum_{JT} (2T + 1)(2J + 1) \langle u_k | V_{NN} | u_p \rangle, \quad (13)$$

where the sum up to the highest occupied orbitals can be converted into integrals up to the Fermi momentum k_F , that is

$$\sum_{u_k, u_p} \langle u_k | V_{NN} | u_p \rangle = \frac{\Omega^2}{(2\pi)^6} \int_0^{k_F} k^2 dk \int d\theta_k \int d\phi_k \int_0^{k_F} p^2 dp \int d\theta_p \int d\phi_p \frac{V_{NN}(\mathbf{k}, \mathbf{p})}{\Omega}. \quad (14)$$

ONCE-ITERATED MATRIX ELEMENTS

The matrix elements of the interaction given in the main text have exactly the same form as Eq. (10) here, by replacing the inner kernel $\langle N' L' M' | \langle n' l' m' | V_{NN} | n l m \rangle | N L M \rangle$ with

$$\frac{1}{4} \sum_{N'' L'' M'' n'' l'' m''} \langle N' L' M' | \langle n' l' m' | V_{iter}^{LO} | n'' l'' m'' \rangle | N'' L'' M'' \rangle \times G \langle N'' L'' M'' | \langle n'' l'' m'' | V_{iter}^{LO} | n l m \rangle | N L M \rangle, \quad (15)$$

where G is given by Eq. (6) in the main text. For a density-independent interaction, the non-vanishing matrix elements in Eq. (15) have quantum numbers $N' = N$, $L' = L$ and $M' = M$. Furthermore, for the s -wave part of the effective interaction $V_{iter}^{LO} = t_0(1 + x_0 P_\sigma)$ considered in this work, we have $n' = n$ and $l' = l = m' = m = 0$ due to the energy conservation property of the Moshinsky transformations. In addition, one can further drop the summation regarding the CM intermediate states $\langle N'' L'' M'' |$ as their overlap is always 1. Thus, the inner kernel (excluding the external $\langle N L M |$ and $| N L M \rangle$)

$$-\frac{m}{4} \frac{(4\pi)^3}{(2\pi)^9} \left[\int_0^{2k_F} K^2 dK \int_0^{k_F} k^2 dk \int_0^\Lambda k'^2 dk' \frac{\Psi_{NLM}^{HO}(K) \psi_{n00}^{HO}(k) [t_0(1 + x_0 P_\sigma)]^2 \psi_{n00}^{HO}(k) \Psi_{NLM}^{HO}(K)}{k'^2 - k^2} \right]_{BC}. \quad (18)$$

The dK integral is not equal to 1 and the denominator does not diverge, due to the fact that the three variables $\mathbf{k} = (\mathbf{k}_1 - \mathbf{k}_2)/2$, $\mathbf{k}' = (\mathbf{k}'_1 - \mathbf{k}'_2)/2 = (\mathbf{k}_1 - \mathbf{k}_2)/2 + \mathbf{q}$, and $\mathbf{K} = \mathbf{k}_1 + \mathbf{k}_2 = \mathbf{k}'_1 + \mathbf{k}'_2$ are restricted by the following BC:

$$\begin{aligned} |\mathbf{k}_1| < k_F, |\mathbf{k}_2| < k_F, \\ |\mathbf{q} + \mathbf{k}_1| > k_F, |\mathbf{k}_2 - \mathbf{q}| > k_F. \end{aligned} \quad (19)$$

A detailed illustration of the above BC and the related treatments to perform the triple integral can be found in Fig.2 and Fig.3 of Ref.[87].

We note that the results for finite nuclei obtained with the above equations correspond to the full expressions given in Eqs. (22) and (27) in Ref.[65] for the EoS. The expressions of second-order EoSs listed in Refs.[61, 63, 64, 78] are the asymptotic form after expanding the results in power series of Λ . Whereas an analytic result of the triple integral can be obtained for the EoS of matter, Eq. (18)

becomes:

$$\begin{aligned} & \frac{1}{4} \sum_{n''00} \langle n00 | V_{iter}^{LO} | n''00 \rangle G \langle n''00 | V_{iter}^{LO} | n00 \rangle \\ & = \frac{1}{4} \sum_{\alpha} \langle n00 | V_{iter}^{LO} | \alpha \rangle G \langle \alpha | V_{iter}^{LO} | n00 \rangle. \end{aligned} \quad (16)$$

Note that we have taken the freedom to re-express the intermediate states from the HO-basis in relative coordinates into any complete set $\sum_{\alpha} |\alpha\rangle \langle \alpha|$ within the same coordinates, where $|\alpha\rangle$ labels the eigenstates. One can then choose the new basis to be the kinetic eigenstates so that $|\alpha\rangle = |u_k\rangle$ and the summation \sum_{α} is converted into an integral over the intermediate momentum k' . At the same time, one can also decompose each outer HO-wavefunction $\langle n00 | k \rangle$ into a linear combination of $\sum_k c_k u_k$, with $c_k = \psi_{n00}^{HO}(k)$. In this way, Eq. (16) becomes

$$-\frac{m}{4} \frac{(4\pi)^2}{(2\pi)^6} \int_0^{k_F} k^2 dk \int_0^\Lambda k'^2 dk' \frac{\psi_{n00}^{HO}(k) [t_0(1 + x_0 P_\sigma)]^2 \psi_{n00}^{HO}(k)}{k'^2 - k^2}. \quad (17)$$

Note that, together with the outer integral on $\langle N L M |$, Eq. (15) becomes

can only be solved numerically for finite nuclei. Although the asymptotic form agrees with the full expression at $\Lambda \rightarrow \infty$, the discrepancies between them can be up to 10% for lower cutoff values ($\Lambda \leq 6 \text{ fm}^{-1}$). Therefore, we always adopt the full expression in the nuclear matter calculations carried out throughout this work.

TABLES OF RENORMALIZED LOW-ENERGY CONSTANTS

We list below the LECs up to NLO based on the prescriptions (i)-(ii) as described in the main text. Note that here C^Λ and $C^{\Lambda*}$ are related to $V^{CT} = C(1 + x_c P_\sigma)$ by

$$\begin{aligned} C &= C^\Lambda \\ x_c &= 1 - \frac{C^{\Lambda*}}{C^\Lambda}. \end{aligned} \quad (20)$$

Λ (fm $^{-1}$)	4	5	6	8	10
t_0 (fm 2)	1.349	-1.732	-2.189	-1.546	-1.307
t_3 (fm $^{2+3\alpha}$)	96.393	40.434	53.091	59.182	60.729
x_0	-2.468	-1.459	-0.188	-0.480	-0.738
x_3	4.188	2.050	0.567	0.479	0.474
α	0.0358	0.218	0.274	0.291	0.289
C^Λ (fm 2)	-10.994	2.578	-0.631	-2.616	-2.241
$C^{\Lambda*}$ (fm 2)	53.597	21.767	5.281	5.208	7.456
χ^2	15.1	30.2	289	334	356

Table II. χ^2 and adjusted parameters based on the prescription (i) obtained for $\Lambda =$ values from 2 to 10 fm $^{-1}$.

Λ (fm $^{-1}$)	4	5	6	8	10
t_0 (fm 2)	-0.173	-0.169	-0.141	-0.0868	-0.139
t_1 (fm 4)	2.448	2.448	2.448	2.448	2.448
t_2 (fm 4)	-2.784	-2.784	-2.784	-2.784	-2.784
t_3 (fm $^{2+3\alpha}$)	69.747	69.747	69.747	69.747	69.747
x_0	-0.243	-0.115	-0.312	1.387	1.387
x_1	-0.328	-0.328	-0.328	-0.328	-0.328
x_2	-1.0	-1.0	-1.0	-1.0	-1.0
x_3	1.267	1.267	1.267	1.267	1.267
α	0.167	0.167	0.167	0.167	0.167
C^Λ (fm 2)	-12.40	-12.398	-12.427	-12.459	-12.410
$C^{\Lambda*}$ (fm 2)	-2.556	-2.579	-2.573	-2.827	-2.605
χ^2	$7.6 \cdot 10^{-3}$	$3.5 \cdot 10^{-3}$	$2.5 \cdot 10^{-3}$	$8.1 \cdot 10^{-4}$	$6.4 \cdot 10^{-4}$

Table III. χ^2 and parameters based on prescription (ii) obtained from $\Lambda = 2$ to 10 fm $^{-1}$. Note that at nuclear matter level we have adopted the empirical EoSs to be those given by the SLy5-mean-field.

The corresponding EoSs generated by LECs listed in Tables II-IV are plotted as Figs.4-6.

Λ (fm $^{-1}$)	4	5	6	8	10
t_0 (fm 2)	-0.183	-0.154	-0.123	-0.069	0.130
t_1 (fm 4)	1.625	1.625	1.625	1.625	1.625
t_2 (fm 4)	-1.710	-1.710	-1.710	-1.710	-1.710
t_3 (fm $^{2+3\alpha}$)	94.811	94.811	94.811	94.811	94.811
x_0	-0.230	-0.099	-0.159	-0.309	1.699
x_1	0.653	0.653	0.653	0.653	0.653
x_2	-0.537	-0.537	-0.537	-0.537	-0.537
x_3	0.181	0.181	0.181	0.181	0.181
α	0.167	0.167	0.167	0.167	0.167
C^Λ (fm 2)	-14.653	-14.678	-14.717	-14.781	-14.849
C^{Λ^*} (fm 2)	-10.263	-10.327	-10.350	-10.410	-10.405
χ^2	$9.7 \cdot 10^{-3}$	$3.5 \cdot 10^{-2}$	$2.4 \cdot 10^{-3}$	$6.1 \cdot 10^{-3}$	$2.2 \cdot 10^{-2}$

Table IV. χ^2 and parameters based on prescription (ii) obtained from $\Lambda = 2$ to 10 fm $^{-1}$. Note that at nuclear matter level we have adopted the empirical EoSs to be those given by the SkP-mean-field.

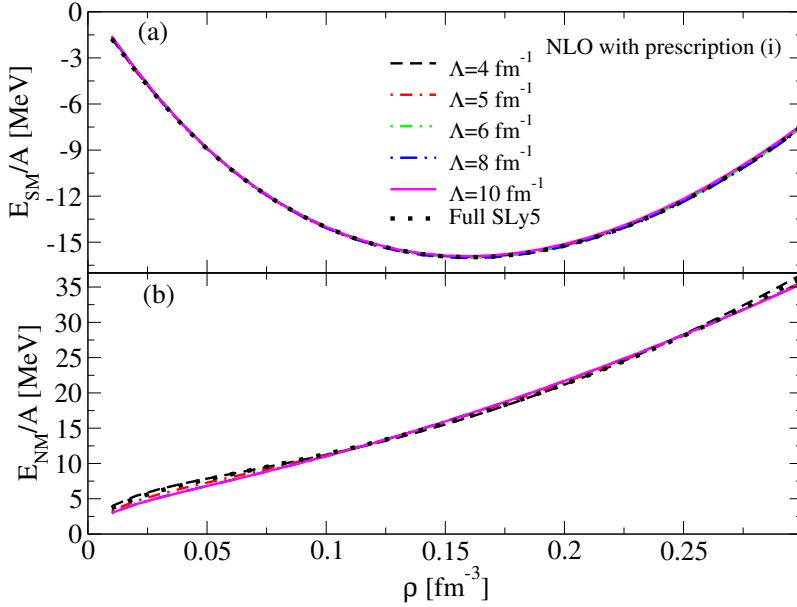


Figure 4. Second-order EOSs for SM (a) and NM (b) under the prescription (i) adjusted on the full SLy5-mean-field EOSs, with an effective mass equal to the bare mass, for different values of the cutoff.

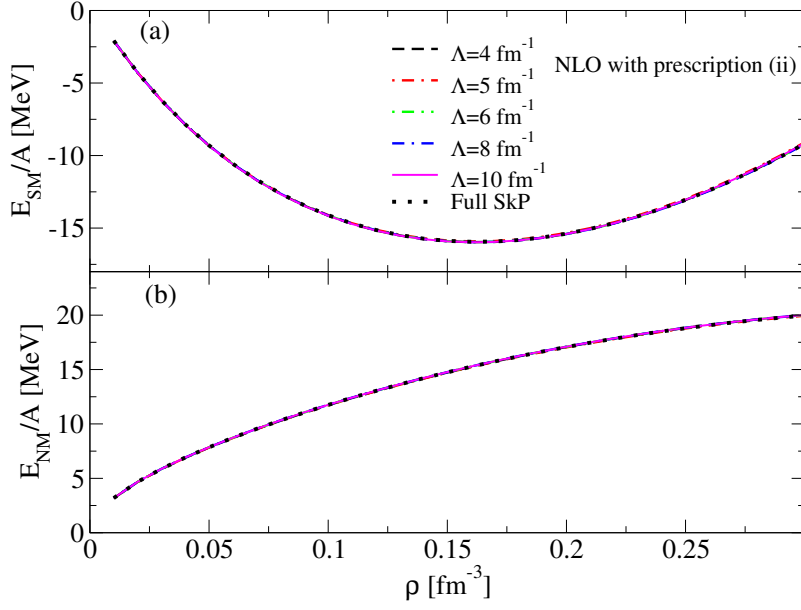


Figure 5. Second-order EOSs for SM (a) and pure NM (b) under the prescription (ii) adjusted on the full SkP-mean-field EOSs, with an effective mass equal to the bare mass, for different values of the cutoff.

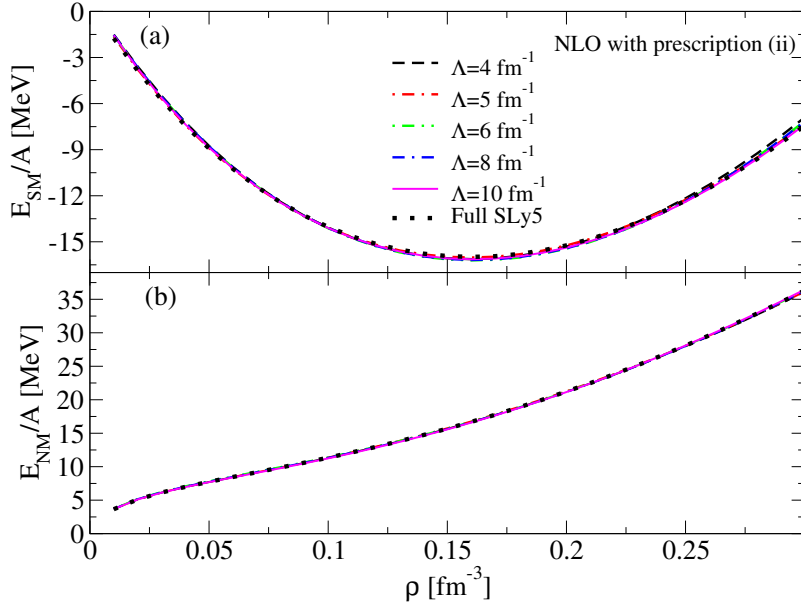


Figure 6. Second-order EOSs for SM (a) and pure NM (b) under prescription (ii) adjusted on the full SLy5-mean-field EOSs, with an effective mass equal to the bare mass, for different values of the cutoff.